

## Inner screening corrections to the Debye interaction in hot/dense plasmas in the vicinity of the bound – free transitions

C. Deutsch<sup>1\*</sup>, G. Naouri<sup>1</sup> and N.A.Tahir<sup>2</sup>

<sup>1</sup>*Gas and Plasma Physics Laboratory, UMR-CNRS 8578, UPS, Paris University, 210, Henri Becquerel Str., 91405, Orsay, France*

<sup>2</sup>*Society for Heavy Ion Research, 1, Plank Str., 64220 Darmstadt, Germany*  
\**e-mail: claude.deutsch@universite-paris-saclay.fr*

Considering hot/dense plasmas strongly ionized and still retaining hydrogenic bound states ( $1 \leq z \leq 6$ ), we focus attention on the delocalization features of ion-electron orbitals, such as wide spreading and attending of pertaining wave functions close to the free bound transition. A systematic embedding process of increasingly excited states is shown to introduce short-range corrections to the Debye potential, while highlighting blue line shifts relative to initial Debye data. D-Dependence of a ion-electron dipole bound in a Debye potential evaluated. The probability of presence  $r_{2R2nl}(r)$  of the electron around its bounding ion are plotted. Orbitals 1S and 2S in a 3-component hydrogen plasma with  $T = 8.62$  eV and  $n_e = 2.24 \times 10^{23} \text{ cm}^{-3}$  are calculated. A classical – partially degenerate difference is shown. Normalized solutions to quantum – mechanical equation for partially ionized hydrogen are obtained. Also levels deeply involved in the bound-free transition, close to vanishing in the continuum are shown.

**Key words:** hot/dense plasmas, bound – free transitions, short-range corrections.

**PACS numbers:** 68.37.-d, 68.90.+g.

### 1 Introduction

It seems that the plasma physics community is presently experiencing a continuous and steadily increasing reassessment of the basic concept, pillars of our discipline. A few salient examples among many, focus on deep and refined re-examination of the Debye screening length altogether with a deep mathematical interpretation of the nonlinear Landau damping [1-4]. Boltzmann – Maxwell equilibria are also under a scrutiny through non-extensive statistical physics [5] featuring non – Maxwellian distributions. These revisitations lead to the introduction of novel perspectives in the whole field of plasma physics, they are often motivated by theoretical breakthroughs in other disciplines. In this context, we do intend to give a specific attention to the remaining Debye bound states in strongly ionized hot/dense plasmas with ion charge  $1 \leq z \leq 6$ .

Considering those hydrogenic levels in the usual temperature Saha – distribution, we then focus on pressure effects, and highlighting the priority of

messy interaction of excited Debye orbitals. As well documented, in contradistinction to the Coulomb spectrum, Debye bound states are finite in number, and the lowest ones could be well approximated as non-degenerate Coulombic. Therefore, a typical electron-ion orbital may be allocated the approximate average extension (a.u.) [6]

$$r_{nl} = \sqrt{\frac{\langle nl | r^2 | nl \rangle a_0}{\langle nl | nl \rangle}} = \frac{1}{2Z} (3n^2 - l(l+1)), \quad (1)$$

with the Bohr radius  $a_0 = 5.29 \times 10^{-9}$  cm already demonstrating a possible inclusion of small orbitals within those endowed with a larger main quantum number, an effect particularly conspicuous for  $l = n-1$ . At this stage it appears fruitful to make contact with a methodology developed in condensed matter physics.

Here, we allude to the systematic embedding of bound orbitals featuring long-range interactions

between dislocations [7, 8], monitored by a 2D Coulomb interaction [9-11]. In this regard, we emphasize hot/dense plasmas with a Debye length ( $n_e$ , electron density)

$$D = \left( \frac{k_B T}{4\pi e^2 (n_e + Z^2 n_z + (Z-1)^2 n_{z-1})} \right)^{1/2} \quad (2)$$

where  $n_z$  is density of fully stripped ions with charge  $Z$ ,  $n_{z-1}$  is density of hydrogenic ions with charge  $Z-1$  and mass  $m_i$ . For the sake of simplicity we restrict ourselves to a 3-component system consisting of electrons, bare ions of nuclear charge

$Z$  in Saha equilibrium and hydrogenic ions of total charge  $Z-1$ .

Those plasmas share an electron plasma parameter

$$\Lambda_e = \frac{\beta e^2}{D_e} = \frac{2.43 \times 10^{-4} n_e (cm^{-3})^{1/2}}{T(^{\circ}K)^{3/2}} \quad (3)$$

with  $D_e$ , electron restriction of Eq.(2).

Then, the extension (1) of the lowest bound orbitals are contrasted in Table I to mean interparticle distance  $R_0$  and electron thermal wavelength.

**Table 1** – Relevant Lengths (in  $a/Z$ ) in Dense Hydrogenic Plasma with Plasma Parameter  $\Lambda_e = 0.7$  (Number of Particles in Debye Sphere 0.23)

$\lambda = 4.09 \times 10^{-5} \left( \frac{\Lambda_e}{D} \right)^{1/2}$	D	Z=1		Z=2		Z=3		Z=4		Z=5		Z=6		nl
		$R_0$	$r_{nl}$	$R_0$	$r_{nl}$	$R_0$	$r_{nl}$	$R_0$	$r_{nl}$	$R_0$	$r_{nl}$	$R_0$	$r_{nl}$	
$2.86 \times 10^{-4}$	4	4.556	1.577 12.370	4.555	1.577 12.582	4.554	1.577 12.813	4.554	1.577 12.813	4.553	1.577 12.883	4.553	1.577 12.937	1s 2s
$3.575 \times 10^{-4}$	5	5.395	1.550 8.6660 8.69834	5.2557	1.550 8.706 9.139	5.176	1.550 8.735 9.241	5.124	1.555 8.755 9.312	5.088	1.555 8.769 9.366	5.061	1.555 8.780 9.407	1s 2s 2p

$r_{nl}$  data are plotted in order of increasing excitation (1s, 2s, 2p, 3s, etc....). The average spatial extension of higher orbitals is clearly larger than  $D$  and  $R_0$ .

It should also be noticed that enhanced  $r_{nl}$  goes hand in hand with large orbiting time  $\sigma_{nl}$ , fulfilling according to the correspondence principle.

$$\sigma_{nl} \frac{Ze^2}{2\pi r_{nl}} = n\hbar, \quad (4)$$

for a pure Coulomb interaction ( $D \rightarrow \infty$ ), while providing a lower bond to corresponding Debye  $\sigma_{nl}$ . We now stress the view, that electron-ion bound pairs can be seen as electric dipoles internally screening the Debye interaction within the biggest dipoles containing them, while simultaneously experiencing the influence of less extended dipoles included by them. One can picture this ordering of embedded electric dipoles as an analog to the familiar Russian puppets (Babushkas) thus mimicking their apparently inextricable entang-

lement. This scenario will then be devoted to a systematic attention in the sequel.

The required Debye-Saha framework is then given attention in Section 2.

A preliminary exposition of the nonlinear resumption process, implying successively embedded dipoles is presented in Section 3 within a classical setting ( $l=0$ ), allowing for the introduction of the dielectric quantity  $\varepsilon(r)$ .

A full quantum-mechanical ( $l \neq 0$ ), extension is laid out in Section 4. Its  $Z$ -dependence is thoroughly examined in Section 5.

Blue line shifts with respect to the red ones featured by the bare Debye potential are demonstrated in Section 6. A summary is finally given in Section 7.

## 2 Debye-Saha framework

The remaining Debye bound states in the above introduced hot/dense 3-component plasma fulfil

$$\left( \beta = \frac{1}{k_B T} \right), \quad (Z-1)n_{Z-1} + Zn_z = n_e, \quad \text{charge}$$

conversation (5)  $\frac{n_{Z-1}}{n_Z} = \left( \frac{h^2}{2\pi m_i k_B T} \right)^{3/2} \frac{n_e e^{\beta I}}{\sum e^{-\beta E_i}}$  Saha  
equilibrium (6)

In terms of ionization potentials

$$I = -E_{1S} + \frac{Ze^2}{D} \quad (7)$$

$E_{1S}$  refers to the ion grand state and  $E_i$  to the remaining discrete spectrum of excited energies. Expression (2) for the Debye length can be usefully reexpressed as

$$D(\text{cm}) = 743 \left( \frac{T(\text{eV})}{n_e(\text{cm}^{-3})(1-\bar{Z})} \right)^{1/2} \quad (8)$$

where

$$\bar{Z} = Z - \frac{n_{Z-1}}{n_e} (Z-1) \quad (9)$$

so that

$$n_{Z-1} = \frac{K n_e / (1 + K(Z-1))}{Z}, \quad K = \frac{n_{Z-1}}{n_Z} \quad (10)$$

reintroduced iteratively in (9) yields a stabilized  $\bar{Z}$  and  $K$  values, altogether with access to the dipole density  $n_{Z-1}$ . Pertaining plasma parameter  $\Lambda_e$  (Eq.(3)) ranges between 0.5 and 1. Time stability of the atomic dipoles is now qualified with respect to the plasma collision time.

$$\sigma_e^{coll} = \frac{2\pi}{\omega_{pe}} = 1.115 n_e^{-1/2} (\text{cm}^{-3}) \quad (11)$$

with  $\omega_{pe}$ , electron plasma frequency.

Moreover, orbiting time of the highest remaining bound orbitals may also be evaluated through the WKB approximation

$$\sigma_{nl(\text{Debye})} = \frac{2\pi m_e}{\partial F_{nl} / \partial n} \quad (12)$$

through a bound state pseudo- analytic expression [12]:

$$E_{nl}(Z, D) = -\frac{h^2}{2m_e D^2} \frac{Z(Z-Z_{nl})}{n^2} \times \left( \frac{Z - A(n+\sigma)^2 + Bn^2}{Z - Z_{nl} + Bn^2} \right) \quad (13)$$

with  $Z_{nl}$  given by  $E_{nl}(Z_{nl}, D) = 0$  (delocalization effect) and

$$A = 1.9765, \sigma = 0.003951, B = 1.2334.$$

It is then appropriate to scale the various considered times with the Coulomb orbiting time

$$\sigma_{nl(cb)} = \frac{2\pi n^2}{Z^2} \times 2.4 \times 10^{-17} \text{ sec}, \quad (14)$$

$$\text{Fulfilling } \frac{\sigma_{nl(\text{Debye})}}{\sigma_e^{coll}} < 1, \text{ any } (n, l), \quad (15)$$

For instance,  $\Lambda_e = 0.7$  with  $D = \frac{4a_0}{Z}$  gives 1.2 for the ratio of the pair (4,3). Therefrom one reaches

$$\frac{\sigma_{nl(\text{Debye})}}{\sigma_e^{coll}} < \frac{n^2}{Z^2} \times 1.353 \times 10^{-12} n_e^{1/2} (\text{cm}^{-3}) \quad (16)$$

and a given  $(n_{\max}, l)$  may be selected out with

$$n_{\max} \leq 10^4 n_e^{-1/6} (\text{cm}^{-3}) Z^{2/3}, \quad (17)$$

So that  $\frac{\sigma_{nl(\text{Debye})}}{\sigma_e^{coll}} \leq 1$  illustrating the collisional

stability of the highest but still bound Debye orbitals. To secure the ingoing renormalization procedure, one is led to assume electric neutrality within every considered arrangement taking place on a  $\sigma_{nl(\text{Debye})}$  timescale, in close analogy with the so-called average atom model (AAM).[13]

### 3 Classical treatment

#### A) Dipole D-Dependence

As a prelude to the systematics of the dipole embedding process, it is of interest to pay a due attention to the D-Dependence of a ion-electron dipole bound in a Debye potential. Figures 1 a,b picture the probability of presence  $r^2 R_{nl}^2(r)$  of the electron around its bounding ion.  $R_{nl}(r)$  denotes the usual Debye and radial wave function herein restricted to low-lying orbits, 1S and 2S in a pretty correlated hydrogen ( $Z=1$ ) plasma with  $T = 8.618$  eV ( $10^5$  K) and  $n_e = 2.24 \times 10^{23} \text{ cm}^{-3}$  Corresponding Fermi temperature  $T_F = 13.462$  eV features a typical case of partial degeneracy – strong coupling plasma, allowing for a vivid illustration of the progressive disappearance of bound orbitals through enhanced

delocalisation when strong coupling and concomitant partial electron degeneracy increase [11].

Those pictures highlight conspicuously swift bound – free transitions of the remaining 1S and 2S bound states (Figures 1 b, d) when the screening length D decays even by a very small amount.

Delocalisation is then signalled by the rather impressive wave function flattening. Those data got derived from the classical Debye interaction  $\frac{e^{-r/D}}{r}$

for a 3-component plasma featuring partial degeneracy ( $T_F > T$ ) because the quantitative difference between the usual interaction and its degeneracy – corrected counterpart [14-16] remains negligible (see Figure 2) for  $r^2 R_{nl}^2(r)$  in the present situation.

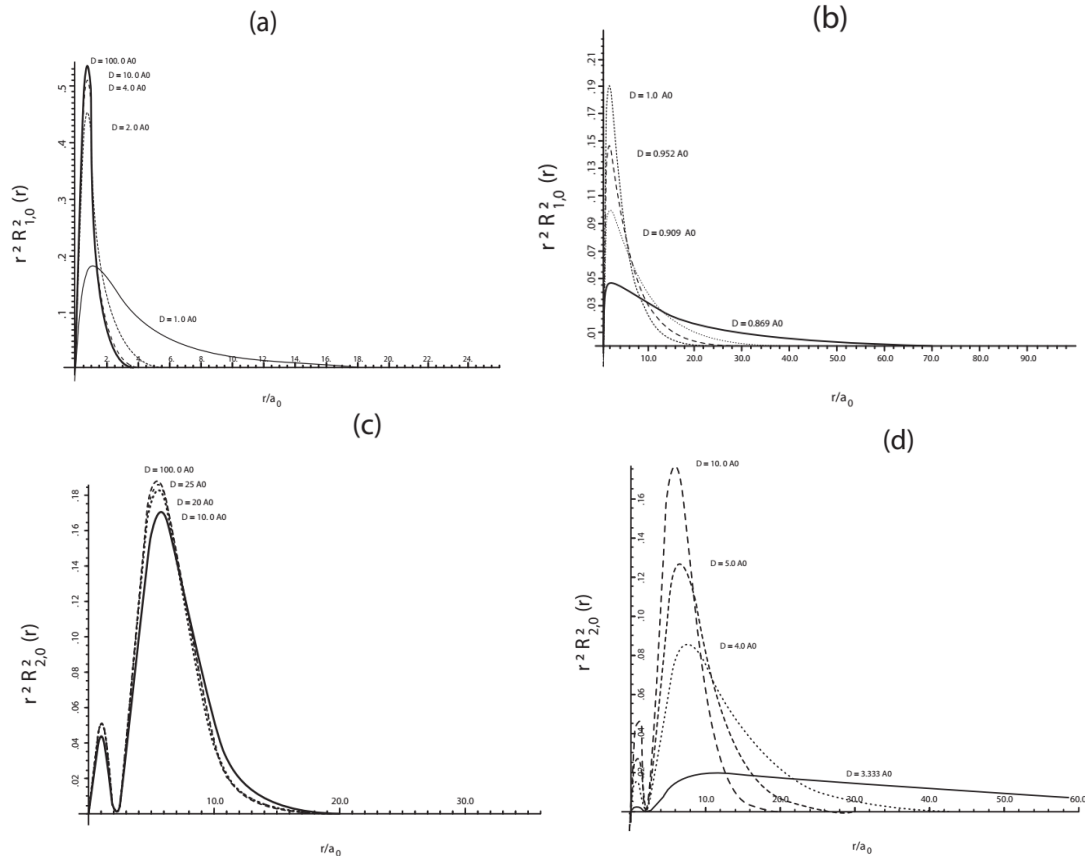


**Figure 1** – Orbitals 1S and 2S in a 3-component hydrogen plasma with  $T = 8.62$  eV and  $n_e = 2.24 \times 10^{23} \text{ cm}^{-3}$ . (a) 1s with  $D=100 \rightarrow 1 a_0$ , (b) 1S with  $D=1 \rightarrow 0.869 a_0$ , (c) 2S with  $D=100 \rightarrow 10 a_0$  and (d) 2S with  $D=10 \rightarrow 3.333 a_0$ .

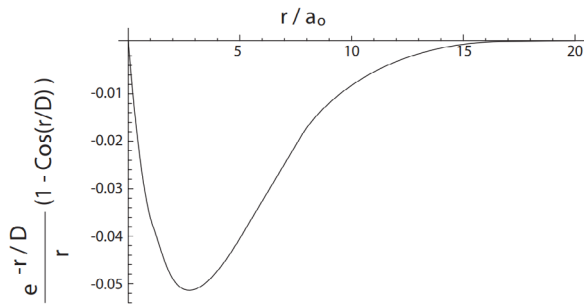


**Figure 2** – Classical – partially degenerate difference

$$\frac{e^{-r/D}}{r}(1 - \cos(r/D)) \text{ for Figures 1 plasma}$$

( $T=8.62 \text{ eV}$ ,  $n_e=2.24 \times 10^{23} \text{ cm}^{-3}$ )

### B) Dipole Embedding

Restricting first to  $l = 0$  states, we initialize the embedding process with the simplifying assumption that every orbitals  $(n,l)$  corresponds to an electric dipole wholly contained in the  $(n', l')$  orbit, whether  $n' > n$ . Recalling also that in moderately coupled plasmas ( $\Lambda_e \leq 1$ ) of present concern, electron exchange effects are only of significance in a relative distance  $\leq 1$  a.u [17], while ion-ion Coulomb interaction remains nonnegligible for interdistances  $\leq 4$ .a.u., we can focus attention on dipole-dipole interactions mimicking superimposed and closed Debye orbitals in a Russian puppet – like arrangement. Then, smaller dipoles of less spatial extension and paced at higher velocity impact those immediately including them through a local dielectric quantity  $\varepsilon(r)$ , fulfilling  $\frac{\varepsilon(r)}{dr} \ll 1$ .

We also emphasize that direct Coulomb interaction within ion fluid may be considered as exactly compensated by the homogeneous free electron background, without noticeable gradient.

So, thermal effects are not expected to produce a significant departure from charge neutrality at the considered dipole level.

Now, we consider the  $(n, l)$  dipole polarisability

$$P(r) = \frac{\partial}{\partial E} \frac{\langle \vec{er}, \vec{E} \rangle}{|\vec{E}|} \Big|_{E=0} \quad (18)$$

with electric charge  $e$  and averaged over instantaneous charge configurations submitted to the Boltzmann statistical factor ( $l = 0$ )

$$e^{-BH} = e^{\beta E \cos \Theta \cdot U(r)}, \quad U(r) = \frac{e^{-r/D}}{\varepsilon(r)r} \quad (19)$$

with a modied screened interaction accounting for the inclusion of enclosed smaller dipoles thus providing additional short-range inner screening to the initially long range one.

Putting Eq.(19) into Eq.(18) yields

$$P(r) = \frac{\beta e^2 r^2}{3}, \quad (20)$$

Then, denoting  $n$  as the overall dipole density, one has  $dn(r)$  dipoles in the  $(r, r + dr)$  range, so that

$$dn(r) = 4\pi n_0^2 \int_r^{r+dr} dr' r'^2 e^{-\beta U(r')} \quad (21)$$

with susceptibility variation  $d\chi = P(r)dn(r)$ , presently restricted to  $l = 0$  states, and satisfying

$$\frac{d\chi}{dr} = n_0^2 \frac{\beta e^2}{3} \times 4\pi r^4 \text{Exp} \left( \frac{\beta e^2}{\varepsilon(r)r} (e^{-r/D} - e^{-r/\zeta}) \right) \quad (22)$$

with an interaction regularized at  $r = 0$ , through electron thermal wavelength.  $n_0$  should be taken large enough to validate the macroscopic relationship  $\chi = (\varepsilon - 1) / 4\pi$ .

Then, introducing  $y = \frac{\beta e^2}{\varepsilon(r)}$  in Eq. (22), leads to the classical and nonlinear relationship

$$\frac{dy}{dr} = \frac{-16n_0^2}{3} \pi^2 y^2 r^4 \text{Exp} \left( \frac{y}{r} (e^{-r/D} - e^{-r/\zeta}) \right) \quad (23)$$

already exhibiting the main characteristics of the following quantum treatment with  $l \neq 0$ . At  $r \rightarrow 0$ ,  $y' \rightarrow 0$ , while  $r \rightarrow \infty$  features the asymptotic result

$$y = \frac{1}{Cr^s / 5 + C_{te}}, \quad (24)$$

$$C = (4\pi)^2 n_0^2,$$

with  $\lim y = 0$  for  $r \rightarrow \infty$ , as depicted in Figure 3.

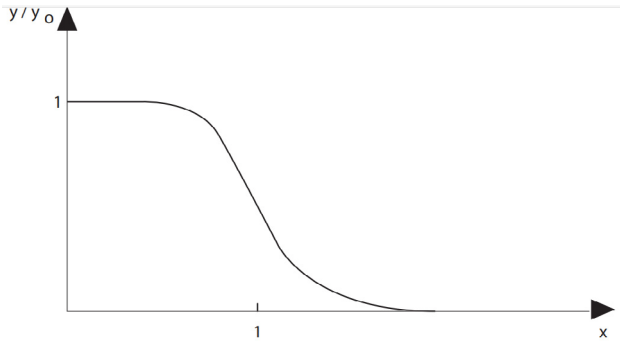


**Figure 3** – Normalized asymptotic solution to the classical relationship (23)

#### 4 Quantum – mechanical treatment ( $l \neq 0$ )

Switching now to any  $l \neq 0$ , we make an intense use of the radial wave function  $R_{nl}(r)$  while securing the dipole density normalization with

$$\int_0^{\infty} dr r^2 R_{nl}^2(r) = 1 \quad (25)$$

Again, the instantaneous number of dipoles writes as

$$dn_{nl}(r) = n_{nl}^2(r) r^2 R_{nl}^2(r) dr, \quad (26)$$

for the  $(n, l)$  dipole density  $n_{nl}$ . It will also convenient to select a given excited orbital  $(n_0, l_0)$ , so every  $(n, l)$  fulfilling  $n < n_0$  or  $l (\leq n-1) < l_0$  provides a contribution to  $\chi_{n_0}$  which reads as

$$d\chi_{n_0}(r) = \sum_{n < n_0, l} dn_{nl}(r) P_l(r) \quad (27)$$

with Saha – distributed excited states,

$$n_{nl} = \frac{n_e^2}{2} \left( \frac{2\pi}{m_e k_B T} \right)^{3/2} e^{\beta(l - E_{nl}^0)} \quad (28)$$

$I$  denotes ionization potential and  $E_{nl}^0$  qualifies the  $(n, l)$  Debye orbital without resummation ( $\varepsilon(r) = -1$ ).

Then, introducing  $n_{nl}$  into  $dn_{nl}(r)$  altogether with  $d\chi_{n_0}(r)$  makes to appear

$$\begin{aligned} \chi_{n_0}(r) &= \\ &= \sum_{n < n_0, l < l_0} \frac{n_e^2}{2} \left( \frac{2\pi \hbar^2}{m_e k_B T} \right)^{3/2} e^{\beta(l - E_{nl}^0)} r^2 R_{nl}^2(r) P_l(r) dr, \end{aligned} \quad (29)$$

with the obvious extension

$$P_l(r) = \frac{\beta^2 r^2}{3} (2l+1), \quad (30)$$

of the classical polarisation. Finally, one reaches

$$d\chi_{n_0}(r) = C \sum_{n < n_0, l} (2l+1) e^{-\beta E_{nl}^0} \frac{\beta e^2 r^4}{3} R_{nl}^2(r) dr, \quad (31)$$

$$\text{where } C = \frac{n_e^2}{2} \left( \frac{2\pi \hbar^2}{m_e k_B T} \right)^{3/2} e^{\beta I}$$

Assigning a function  $E_{n_0}(r)$  to every  $\chi_{n_0}(r)$ , so that  $y_{n_0}(r) = \frac{1}{E_{n_0}(r)}$  yields access to

$$\begin{aligned} dy(r) &= -\frac{4\pi}{3} C e^2 r^4 y_{n_0}^2(r) \times \\ &\times \sum_{n < n_0, l} (2l+1) e^{-\beta E_{nl}^0} R_{nl}^2(r) dr \end{aligned} \quad (32)$$

obvious quantum – mechanical extension of Eq. (23), pictured on Figure 4, where level 3p experiences inner screening from It is very important to notice the nearly  $y_{nl}(r)$  constant behavior, in particular at large  $r/a_0$  value. Also, the Debye ionization limit does not get shifted by the present renormalization. Levels  $(n, l)$  are likely to experience larger blue shift than lower ones, with respect to the unperturbed Debye value ( $\varepsilon(v) = 1$ ).

#### 5 Dependence

Enlarging the above exploration to a Z-dependent (see Figure 5) scanning unravels global trends encapsulated in Eq.(32).

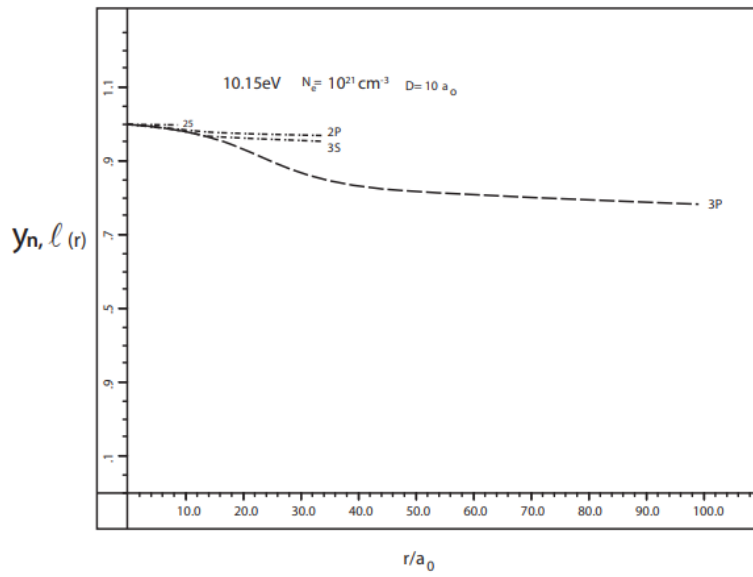


**Figure 4** – Normalized solutions to quantum – mechanical Eq. (32) for partially ionized hydrogen. 3S. This latter being in turn inner-screened from 2P and so on, in a hot/dense and partially ionized hydrogen plasma.

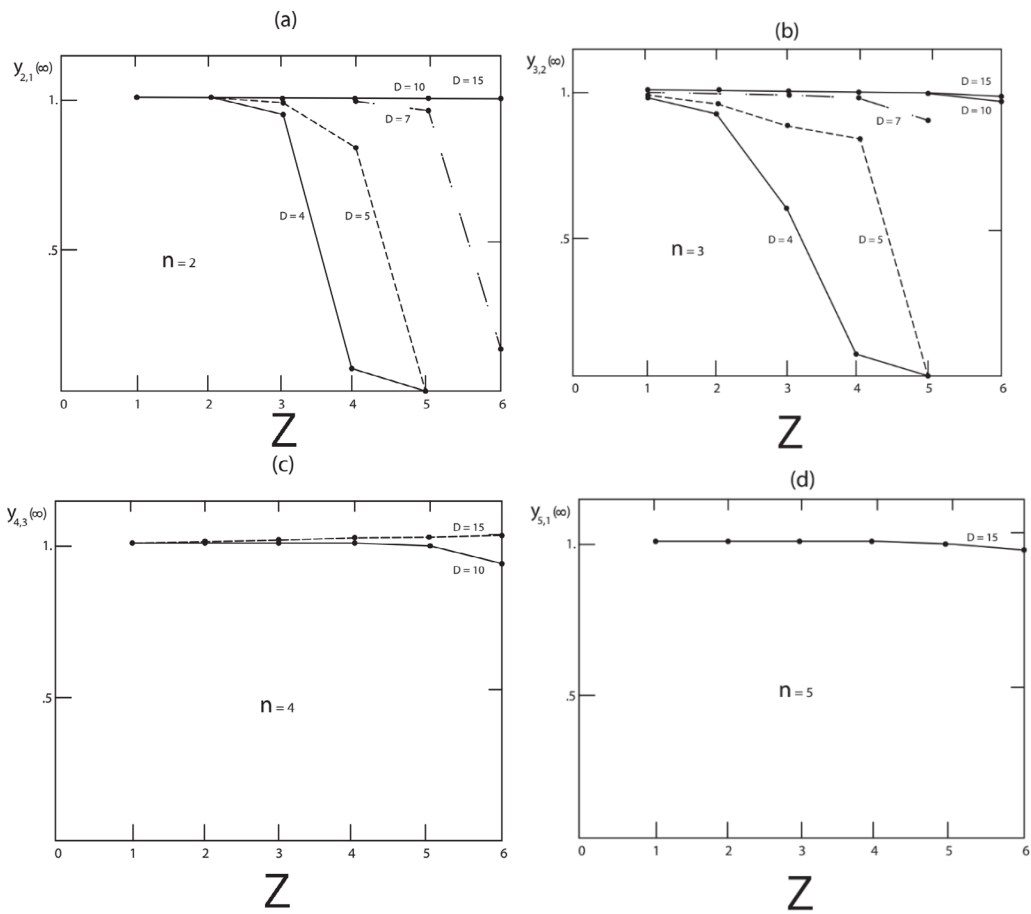


**Figure 5** – Asymptotic renormalisation factor  $y_{n,n-1}(\infty)$  in terms of ion charge  $Z$  hydrogenic main quantum number  $n$  for (a)  $n=2$ , (b)  $n=3$ , (c)  $n=4$  and (d)  $n=5$  with  $D$  in  $a_0/Z$  in hot/dense plasmas with  $n_e = 10^{23}\text{cm}^{-3}$

**Table 2** – Asymptotic renormalisation factor  $y_{n, n-1(\infty)}$  for the Debye potential in terms of main quantum number  $n$  and ion echarge  $z \leq 6$  in hot / dense plasmas with  $n_e = 10^{23} \text{ cm}^{-3}$  and Debye length  $D$  ( $a_0/z$ ). Missing entries qualify continuum states(a)  $Z=1 \text{ H}$ 

$y_{n, n-1(\infty)}$	$n=2$	$n=3$	$n=4$	$n=5$	$T \text{ (eV)}$
D=4	0.999	0.983			51.34
D=5	0.999	0.988			80.234
D=7	0.999	0.998			157.242
D=10	0.999	0.999	0.998		320.9363
D=15	0.999	0.999	0.999	0.997	722.134

(b)  $Z=2 \text{ He}$ 

$y_{n, n-1(\infty)}$	$n=2$	$n=3$	$n=4$	$n=5$	$T \text{ (eV)}$
D=4	0.997	0.927			60.91
D=5	0.999	0.960			95.18
D=7	0.999	0.996			186.55
D=10	0.999	0.999	0.994		320.704
D=15	0.999	0.999	0.999	0.993	855.72

(c)  $Z=3 \text{ Li}$ 

$y_{n, n-1(\infty)}$	$n=2$	$n=3$	$n=4$	$n=5$	$T \text{ (eV)}$
D=4	0.950	0.600			36.1
D=5	0.995	0.882			56.40
D=7	0.999	0.992			110.55
D=10	0.999	0.999	0.989		225.60
D=15	0.999	0.999	0.998	0.998	507.61

(d)  $Z=4 \text{ Be}$ 

$y_{n, n-1(\infty)}$	$n=2$	$n=3$	$n=4$	$n=5$	$T \text{ (eV)}$
D=4	0.049				25.38
D=5	0.844				36.66
D=7	0.998	0.981			77.73
D=10	0.999	0.998	0.982		158.63
D=15	0.999	0.999	0.998	0.982	356.91

(e)  $Z=5 \text{ B}$ 

$y_{n, n-1(\infty)}$	$n=2$	$n=3$	$n=4$	$n=5$	$T \text{ (eV)}$
D=4	0.00				19.49
D=5	0.011				30.46
D=7	0.958	0.906			59.69
D=10	0.999	0.997	0.969		121.83
D=15	0.999	0.998	0.997	0.974	274.107

(f)  $Z=6 \text{ C}$ 

$y_{n, n-1(\infty)}$	$n=2$	$n=3$	$n=4$	$n=5$	$T \text{ (eV)}$
D=4					15.79
D=5					24.6735
D=7	0.168				48.36
D=10	0.996	0.990	0.907		98.70
D=15	0.999	0.999	0.996	0.953	222.08

Now we can contemplate the overall nearly constant and plateau-like behavior of the renormalisation factor (RF)  $y_{n,l}(r)$ .

$y_{n, n-l(\infty)}$  data pertaining to the highest  $n$ -dependent RF are systematized in Figures 5 and Table 2. for a varying ion charge  $Z \leq 6$  in hot/dense plasmas with  $n_e = 10^{23} \text{ cm}^{-3}$ .

Corresponding temperature data  $T(\text{eV})$  are sorted according to  $D$  values in  $a_0/Z$ . The larger  $n$ , the larger  $y_{n, n-l(\infty)}$ , thus featuring a stabilized dielectric function  $\varepsilon_{nl}(r)$  at large distance  $r$ . This trend gets amplified for decreasing  $D$  values, advocating a larger wave function delocalisation. It grows nonlinearly with increasing  $Z$  (Figures 5 a, b).

Small RF data correspond to levels deeply involved in the bound-free transition, close to vanishing in the continuum.

Highly excited bound states  $n=4,5$  survive only with  $D=10,15$  in  $a_0/Z$ , thus vindicating a rather weak renormalisation effect only (Figures 5 c, d).

The dipole density vanishes at  $r=0$ , so  $y_{n,l}(0)=1$  and  $y_{n,l}(r) \rightarrow 0$  at  $r \rightarrow \infty$

It should also be appreciated that it proves rather difficult to pursue the present line of reasoning beyond  $Z=6$  and  $D \leq 15 a_0/Z$ , because pertaining plasma parameter  $\Lambda_e$  turns  $\gg 1$ .

So, the Saha level distribution loses progressively its meaning while  $y_{n, n-l}(r) \rightarrow 0$  rapidly. Moreover increasing  $Z$  without bound makes the wave function more and more hydrogenic [20 – 21], so that it exhibits less and less delocalisation.

## 6 Blue line shift

The presently considered renormalisation process makes to appear a more global perspective when one focusses on wavelength relative shift  $-\frac{\Delta\lambda}{\lambda}$  in terms of ion charge  $Z$  and electron plasma

$$\text{parameter } \Lambda_e = \frac{\beta e^2}{D_e}.$$

Required parameters investigation makes use of Schrodinger eigenquantities derived from [18] and [19] codes conveniently initialized with analytic eigenquantities pertaining to modified Hulthen potential [16],

$$V(v) = \frac{-Zg e^{-gr}}{1 - e^{-gr}} + \frac{l(l+1)}{2} \left( \frac{g}{1 - e^{-gr}} \right)^2 e^{-gr},$$

$$g = \frac{1}{D} \ln \frac{a_0}{Z} \quad (33)$$

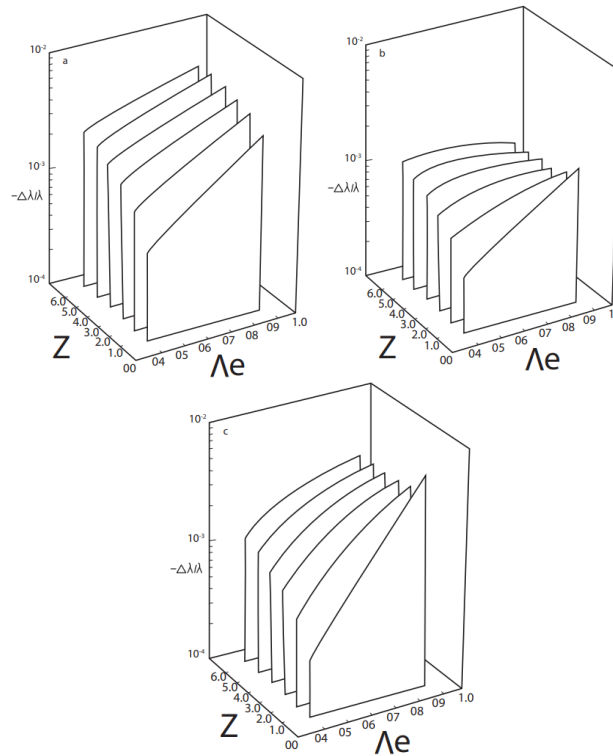


**Figure 6** – Relative wavelength shifts relative to the Debye one ( $\varepsilon(r) = 1$ ) for various conditions as function of  $Z$  and  $\Lambda_e$ . (a)  $Ly_\infty$  and  $D=5a_0/Z$ ; (b)  $Ly_\beta$  and  $D=10a_0/Z$ ; (c)  $Ly_\infty$  and  $D=10a_0/Z$ .

Blue relative shifts  $> 10^{-3}$  are obtained with respect to the unperturbed Debye ones ( $\varepsilon(\nu)=1$ ). They are significantly larger than those seen in weakly coupled plasmas ( $\Lambda_e < 0.1$ ) [22] which result from distinct temperature – dependent mechanisms.

Presently considered  $Ly_\infty$  and  $Ly\beta$  shift increase with  $Z$  and  $\Lambda_e$ , in the hydrogenic sequence. The optimum  $\Lambda_e$  value for which the last bound state disappears into the continuum, remains below unity. These are negative shifts with respect to the overall Debye red shift. Such a trend increasing steadily with  $Z$  and  $\Lambda_e$ , thus provides reduction of the usual Debye shift, recognized as oversized.

## 7 Conclusions

Focussing attention on strongly ionized, hydrogenic hot/dense plasmas and triggered by the observation that radial wave function of Debye bound states experience a marked delocalisation

process in the vicinity of bound – free transitions we have elaborated a systematic iterative embedding of electron – ion orbitals increasingly excited. We have been led to develop a 3D quantum – mechanical extension of an analogous classical process initiated in low dimensional condensed matter physics [7-10].

The key quantity featuring the conspicuous embedding process is the renormalisation factor  $y_{\lambda,n}(r)$ , inverse of the orbitals dielectric function, qualifying local electric dipoles. Corresponding charge  $Z$  dependence is shown as strongly nonlinear, for  $Z \leq 6$ . A salient by – product of this investigation advocates a significant reduction of the usual real line shift typical of the Debye potential and usually considered as too large. Up to now, we restricted attention to moderately correlated and dense plasmas with electrons taken classical. It then remain to pay a due attention to more strongly coupled hydrogenic plasmas neutralized by a partially degenerate electron fluid.

## References

1. Livadiotis G. On the generalized formulation of Debye shielding in plasmas // *Phys. Plasmas.* – 2019. – V. 26. – P.050701.
2. Liu Y.L, Li C.L. A generalized Debye – Huckel theory of electrolyte solutions // *AIP Advances.* – 2019. – P.015214.
3. Janev R.K., Zhang S., J. Wang. Review of quantum collision dynamics in Debye plasmas. // *Matter and Radiation at Extremes.* – 2016. – V.1. –P. 237.
4. Villani C. Particles systems and nonlinear Landau damping // *Phys. Plasmas.*- 2014. – V. 21. – P.03090.
5. Linares J.A.S., Sliva R., Santos J. Plasma oscillations and nonextensive statistics // *Phys.Rev.* – 2000. – V. E61. – P. 3260.
6. Bethe H.A., Salpeter E.E. Quantum mechanics of one and two-electron atoms. NY: Rosetta Publ, plenum Press,1977.
7. Berezinskii V.L. Destruction of long-range order in 1D and 2D systems possessing a continuous symmetry group // *II Quantum systems Sov.Phys.* – 1972. – V. JETP34. – P.610.
8. Ryzhov V.N, Tareyeva E.E., Fomin Yu D., Tsiok E.N. Berezinskii – Kosterlitz – Thouless transition and D melting // *Phys.USP.* – 2017. – V. 60. – P.857.
9. Kosterlitz J.M., Thouless D.J. Ordering, metastability and phase transitions in 2D systems // *J.Phys.* – 1973. – V.C6. – P.1181.
10. Wilson K.G. The renormalization group and critical phenomena // *Rev.Mod.Phys.* – 1983. – V.55. – P.833.
11. Deutsch C., Lavaud M. Equilibrium properties of a 2D Coulomb // *Phys.Rev. A.* – 1974. – V.9. – P.2598.
12. Green A.E.S. Energy eigenvalues for Yukawa potentials // *Phys.Rev. A.* – 1982 – V. 26. – P.1759.
13. Fromy P., Deutsch C., Maynard G. Thomas – Fermi-like and average atom models for dense and hot matter // *Phys. Plasmas.* – 1996. – V.3. – P. 714.
14. Rogers F., Graboske H.C., Harwood D.J. Bound eigenstates of the screened Coulomb potential // *Phys.Rev.* – 1970. – V.A1. – P.5777.
15. Grandjouan N., Deutsch C. Two-body sun over states of the static screened Coulomb potential // *Phys.Rev.* – 1978. – V. A17. – P.795.
16. Shukla P.K., Eliasson B. Screening and wake potentials in quantum plasmas // *Phys.Lett. A.* – 2008. – V. 372. – P.2877.

17. Dharma-Wardana M.W.C, Perrot F., Aers G.C. Effective proton-proton potential in hydrogen plasmas // Phys. Rev. -1983. –V. 28. – P.344.
18. Truhlar D.G. Finite difference boundary value method for solving one -dimensional eigenvalue equation // J.Compt.Phys.- 1972. – V.10. – P.233.
19. Cooley J.W. An improved eigenvalue corrector for solving the Schroedinger equation for central elds // Math. Comm. – 1961. – V.15. – P.363.
20. Green R.L., Aldrich C. Variational wave functions for a screened Coulomb potential // Phys. Rev. A. – 1976. – V.14. – P.2363.
21. Lam C.S, Varshni Y.P. Energies of eigenstates in a static screened Coulomb potential // Phys Rev. A. – 1971. – V.4. – P.1875.
22. Nguyen H., Koenig M., Benredjem D., Caby M., Coulaud G. Atomic structure and polarization line shift in dense and hot plasmas // Phys. Rev. A. – 1986. – V. 33. – P. 1279.